Research Article

# Human Coronavirus 229E Remains Infectious on Common Touch Surface Materials

Sarah L. Warnes, Zoë R. Little, C. William Keevil

*Rita Colwell, Editor*

**DOI:** 10.1128/mBio.01697-15

## ABSTRACT

The evolution of new and reemerging historic virulent strains of respiratory viruses from animal reservoirs is a significant threat to human health. Inefficient human-to-human transmission of zoonotic strains may initially limit the spread of transmission, but an infection may be contracted by touching contaminated surfaces. Enveloped viruses are often susceptible to environmental stresses, but the human coronaviruses responsible for severe acute respiratory syndrome (SARS) and Middle East respiratory syndrome (MERS) have recently caused increasing concern of contact transmission during outbreaks. We report here that pathogenic human coronavirus 229E remained infectious in a human lung cell culture model following at least 5 days of persistence on a range of common nonbiocidal surface materials, including polytetrafluoroethylene (Teflon; PTFE), polyvinyl chloride (PVC), ceramic tiles, glass, silicone rubber, and stainless steel. We have shown previously that noroviruses are destroyed on copper alloy surfaces. In this new study, human coronavirus 229E was rapidly inactivated on a range of copper alloys (within a few minutes for simulated fingertip contamination) and Cu/Zn brasses were very effective at lower copper concentration. Exposure to copper destroyed the viral genomes and irreversibly affected virus morphology, including disintegration of envelope and dispersal of surface spikes. Cu(I) and Cu(II) moieties were responsible for the inactivation, which was enhanced by reactive oxygen species generation on alloy surfaces, resulting in even faster inactivation than was seen with nonenveloped viruses on copper. Consequently, copper alloy surfaces could be employed in communal areas and at any mass gatherings to help reduce transmission of respiratory viruses from contaminated surfaces and protect the public health.

**IMPORTANCE** Respiratory viruses are responsible for more deaths globally than any other infectious agent. Animal coronaviruses that “host jump” to humans result in severe infections with high mortality, such as severe acute respiratory syndrome (SARS) and, more recently, Middle East respiratory syndrome (MERS). We show here that a closely related human coronavirus, 229E, which causes upper respiratory tract infection in healthy individuals and serious disease in patients with comorbidities, remained infectious on surface materials common to public and domestic areas for several days. The low infectious dose means that this is a significant infection risk to anyone touching a contaminated surface. However, rapid inactivation, irreversible destruction of viral RNA, and massive structural damage were observed in coronavirus exposed to copper and copper alloy surfaces. Incorporation of copper alloy surfaces in conjunction with effective cleaning regimens and good clinical practice could help to control transmission of respiratory coronaviruses, including MERS and SARS.

## INTRODUCTION

Treatment of infectious disease is currently facing a crisis. Widespread antibiotic resistance has reduced therapeutic options against bacterial pathogens. However, there is also a significant threat

from reemerging, newly evolving, and zoonotic viral pathogens. In addition, new technologies are also able to identify previously unknown pathogenic viruses. The majority of these are RNA viruses transmitted through the mucosal or respiratory route and manifesting as respiratory disease (1). Respiratory viruses can cause a wide range of lung disorders ranging from mild upper respiratory tract infections to more-severe life-threatening pathologies, including bronchiolitis, fever, pneumonia, and acute respiratory distress syndrome. The World Health Organization (WHO) estimated that there are 450 million cases of pneumonia per year resulting in 4 million deaths, and approximately 200 million of these are cases of viral community-acquired pneumonia (reviewed in reference 2). Common viruses include respiratory syncytial virus (RSV), rhinoviruses, influenza virus, parainfluenzavirus, and coronaviruses. Coinfections with two or more pathogens and comorbidities often affect disease severity and prognosis and complicate initial diagnosis (3).

Many coronavirus species are important animal pathogens and are often host species specific. In humans, several species, e.g., human coronavirus 229E (HuCoV-229E) and NL63 (*Alphacoronavirus*) and HKU1 and OC43 (*Betacoronavirus*), are a common cause of upper respiratory tract infection. There is an ever-present risk of pathogens emerging from animal reservoirs that have attained the ability to infect humans. The risk can be increased when individuals have continuous and close contact with animals; also, climate changes can change the distribution of insect vectors and hosts (4, 5).

In 2003, a highly pathogenic coronavirus believed to have originated in bats and palm civet cats transferred to humans in Guangdong Province, China, resulting in cases of severe acute respiratory syndrome (SARS). Over 8,000 people were infected in 37 different countries, but mostly in Southeast Asia, with 10% mortality. Inefficient human-to-human transmission, severe restrictions on air travel, closure of many wild-animal markets, and quarantine procedures have successfully contained the outbreak so far. However, zoonotic transmission of a coronavirus from reservoirs in bats and possibly camels gave rise to severe respiratory infection in individuals in the Arabian Peninsula in 2012. The resulting Middle East respiratory syndrome (MERS), which affects the lower respiratory tract, is clinically similar to SARS but pathologically different. A ubiquitous host cell receptor often leads to extrapulmonary disease, often in the kidneys, and viral progeny are released through apical and basolateral respiratory cell surfaces, contributing to the high (up to 40%) mortality rate (reviewed in references 6 and 7). Late uncontrolled inflammation leads to severe pathologies which are not dependent on viral load, and human-to-human spread does occur (reviewed in references 3 and 4). This, combined with a low infectious dose, suggests that transmission of very few virus particles via person-to-person or contact with contaminated surfaces may be an infection risk. Although camels and associated food products have been found to contain the virus, a recent study of individuals constantly in contact with infected herds suggested that zoonotic transmission is rare (8) but that the risk may be highest from juvenile animals. The risk of transmission is increased, however, in clinical facilities (9) and possibly in other crowded public areas, including care homes and areas of mass gatherings, such as the Hajj Muslim pilgrimage to Mecca. In a recent outbreak in South Korea, MERS has so far (July 2015) killed 36 people and infected 186 patients in hospital-associated cases associated with the first imported case arising from travel to the Middle East (10, 11).

Surface contamination has recently been found to be more significant than originally thought in the spread of many diseases (12). Symptoms of respiratory disease often result in continuous recontamination of surfaces which are then touched, and infectious virus particles may be transferred to facial mucosa. In addition, ineffective cleaning agents may leave residual particles that can initiate infection (13). The use of biocidal surfaces may help to reduce the incidence of infections

spread by touching contaminated surfaces. Copper alloys have demonstrated excellent antibacterial and antifungal activity against a range of pathogens in laboratory studies (14–19). Copper ion release has been found to be essential to maintaining efficacy, but the mechanism of action is variable (20, 21). A reduction in microbial bioburden and acquisition of nosocomial infection has now been observed in clinical trials of incorporation of copper alloy surfaces in health care facilities (22–25).

Previous studies have shown that murine norovirus (MNV) and human norovirus, highly infectious nonenveloped viruses that are resistant to environmental stress and impervious to many cleaning agents, are destroyed on copper and copper alloy surfaces (26–28). HuCoV-229E is associated with a wide range of respiratory disease from mild colds to severe pneumonia in immunocompromised people and has been implicated as an autoimmune trigger in multiple sclerosis (29, 30). Infection with this virus occurs in a high proportion of the population in approximately 3-year cycles, incurring considerable hidden costs in lost work hours, and in this study was also used as a surrogate for the more virulent coronaviruses responsible for SARS and MERS (rather than using animal viruses or coronaviruses that primarily infect the gastrointestinal tract). In addition, a recent study also observed that HuCoV-229E shares important characteristics with MERS-coronavirus and also has an ancestral link with bats (31). In this study, the ability of HuCoV-229E to retain infectivity on a range of common surface materials was investigated to understand the risk of disease dissemination. The potential use of biocidal surfaces to provide constant antiviral activity against continual surface recontamination could help to limit the spread of respiratory viruses; accordingly, the efficacy of a range of copper alloys to inactivate HuCoV-229E was also determined.

## RESULTS

**Coronavirus persists in an infectious state on common surface materials for several days.** An inoculum of $10^3$ plaque forming units (PFU) persisted on polyfluorotetraethylene (Teflon; PTFE), polyvinyl chloride (PVC), ceramic tiles, glass, and stainless steel for at least 5 days (and 3 days for silicon rubber) at 21°C and a relative humidity of 30% to 40% (Fig. 1).

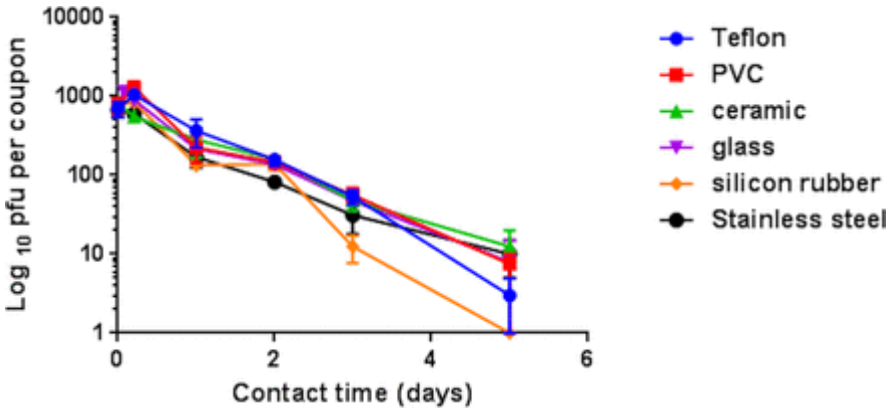


**FIG 1**

Persistence of infectious human coronavirus on common surface materials. Approximately $10^3$ PFU HuCoV-229E (20 µl infected-cell lysate) was applied to 1-$cm^2$ coupons of test surface materials and incubated at ambient conditions (21°C; relative humidity, 30% to 40%). Virus was removed and assayed for infectivity at various time points as described in the text. Although the initial inoculum concentration was quite low, the virus retained infectivity for 5 days on all surfaces, except silicon rubber. Therefore, natural contamination of common surface material with very few coronavirus particles could represent a considerable risk of infection spread if touched and transferred to facial mucosa. Error bars represent ± SEM, and data are from the results of multiple experiments.

**Rapid inactivation of human coronavirus occurs on brass and copper nickel surfaces at room temperature (21°C).**Brasses containing at least 70% copper were very effective at inactivating HuCoV-229E (Fig. 2A), and the rate of inactivation was directly proportional to the percentage of copper. Approximately $10^3$ PFU in a simulated wet-droplet contamination (20 µl per $cm^2$) was inactivated in less than 60 min. Analysis of the early contact time points revealed a lag in inactivation of approximately 10 min followed by very rapid loss of infectivity (Fig. 2B). As observed previously for norovirus, zinc demonstrated a slight antiviral effect compared to that seen with stainless steel (neither metal contains copper).

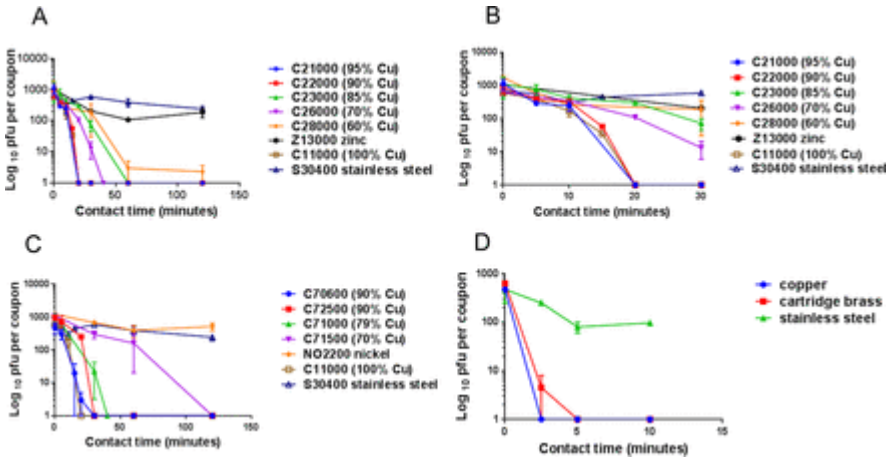


**FIG 2**

Rapid inactivation of human coronavirus occurs on brass and copper nickel surfaces. Approximately $10^3$ PFU HuCoV-229E (20 µl infected-cell lysate) was applied to 1-$cm^2$ coupons of a range of brasses (A and B [early time points only]), copper nickels (C), and control metal surfaces that did not contain copper (stainless steel, zinc, and nickel). Virus was removed at various time points and assayed for infectivity as described in the text. Coronavirus was inactivated in ≤40 min on brasses and 120 min on copper nickels containing less than 70% copper. Analysis of the initial 30 min of contact between virus and brasses (Fig. 2B) reveals an initial lag followed by rapid inactivation. Stainless steel and nickel did not demonstrate any antiviral activity, although mild antiviral activity was observed on zinc (this was significant only at 60 min [$P = 0.046$]). (D) The same inoculum was applied as 1 µl/$cm^2$, was dried immediately to simulate fingertip touch contamination, and was found to have inactivated the virus approximately 8 times faster. Error bars represent ± SEM, and data are from the results of multiple experiments.

Copper nickels were also effective at inactivating HuCoV-229E but required higher (90%) copper content to produce a degree of inactivation equivalent to that seen with brasses containing 70% copper (Fig. 2C). The inactivation time was reduced further in the rapidly drying fingertip contamination model by approximately 8-fold to 5 min for C26000 cartridge brass (Fig. 2D).

Using the same data for simulated droplet contamination, a comparison between brasses and copper nickels containing the same percentage of copper, 90% or 70%, is demonstrated in Fig. 3. At the higher copper content level, there was little difference in efficacy between C22000 and C70600 (Fig. 3A). However, copper nickel C72500 was less effective than C70600 although it contains the same percentage of copper. The superior antiviral properties of C70600 have been observed previously for norovirus and may involve the cuprous oxide layer visible as a removable layer (27). However, at a lower percentage of copper, the cartridge brass was far superior to copper nickel C71500, inactivating virus in approximately one-third the time (Fig. 3B).

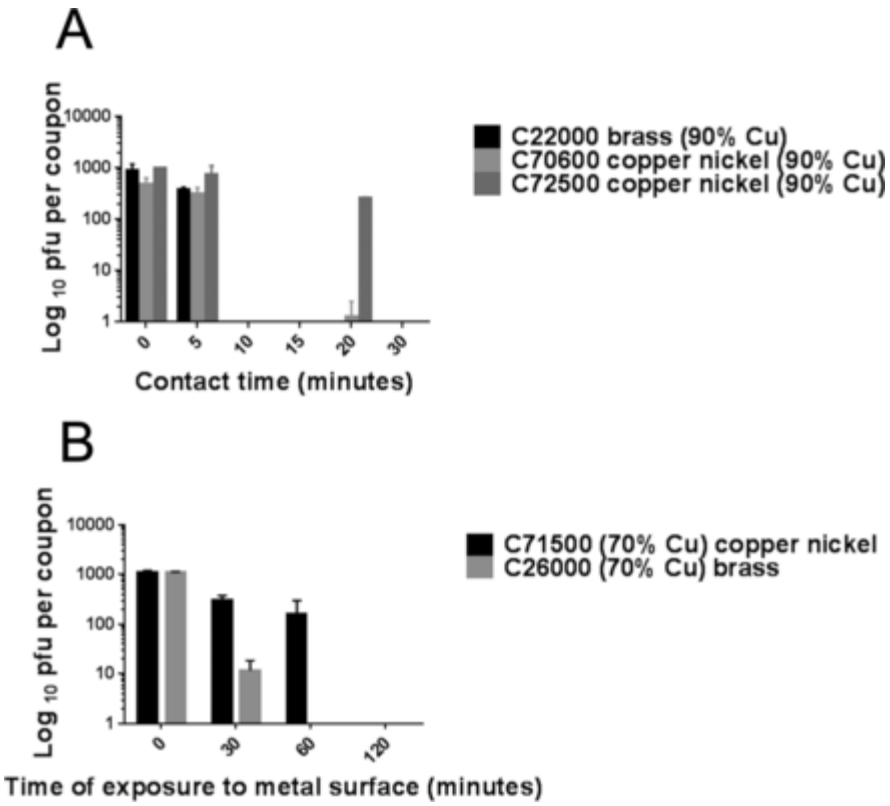


**FIG 3**

Comparison between brasses and copper nickels (containing the same percentage of copper) used to inactivate human coronavirus to determine if zinc content enhances the antiviral effect. Approximately $10^3$ PFU was inoculated onto alloys containing 90% copper for 0, 5, and 20 min (A) or 70% copper for 0, 30, and 60 min (B) and was then removed and assessed for infectivity as described in the text. Alloys containing 90% copper were very effective at inactivating human coronavirus (A), but variations in efficacy did not appear to be related only to the presence of zinc. The presence of copper nickel C70600 resulted in increased efficacy compared to that of copper nickel C72500; that result may be linked to surface oxide layer or copper ion release from this alloy. However, at a lower percentage of copper (B), synergy with zinc or Cu(I) release may be important because contact with cartridge brass resulted in virus inactivation that was at least 3 times faster than that seen with copper nickel C71500.

**Copper ion release and generation of reactive oxygen species (ROS) are involved in inactivation of HuCoV-229E on copper and copper alloy surfaces.**HuCoV-229E was inoculated onto copper and cartridge brass surfaces (100% and 70% copper, respectively; **Table 1**) in the presence of ethylenediaminetetraacetic acid (EDTA) and bathocuproine disulfonate (BCS), chelators of Cu(II) and Cu(I), respectively. Both chelators initially protected the virus from inactivation for up to 2 h (although BCS was still protective after 2 h of contact with brass) (**Fig. 4A** and **C**). This suggests that both ionic species of copper are required directly and/or indirectly for virus inactivation and that Cu(I) may be more significant in the longer term.

**TABLE 1**

Composition of metal alloys used for the study

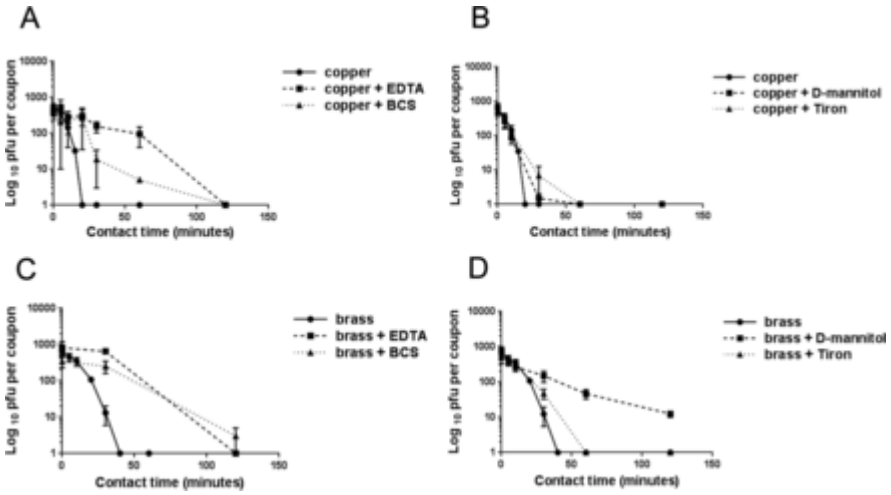


**FIG 4**

Inactivation of coronavirus on copper and cartridge brass surfaces in the presence of chelators EDTA and BCS (A and C) and quenchers d-mannitol and Tiron (B and D) to remove Cu(II) or Cu(I) ionic species and hydroxyl radical or superoxide, respectively. Both chelators protected coronavirus from inactivation on copper and brass surfaces, suggesting that release of Cu(I) and Cu(II) is required for antiviral activity. Tiron was protective for the first hour of contact on copper and brass surfaces, indicating that superoxide is directly or indirectly involved in the inactivation mechanism. However, d-mannitol gave minimum protection on copper but prolonged protection on brass surfaces. Increasing the concentration of d-mannitol did not affect the results (not shown). This suggests that copper ions are the main moieties responsible for inactivation of coronavirus on 100% copper surfaces but that generation of hydroxyl radicals becomes more significant as the concentration of copper in the alloy is reduced. EDTA, BCS, d-mannitol, and Tiron did not significantly affect the infectivity of HuCoV-229E on stainless steel controls or in suspensions (not shown). Error bars represent ± SEM, and data are from the results of multiple experiments.

Inoculation of coronavirus in the presence of d-mannitol and Tiron (4,5-dihydroxy-1,3-benzene disulfonic acid) to quench hydroxyl radicals and superoxide anions, respectively, was done to determine if these moieties were involved in the coronavirus inactivation mechanism (**Fig. 4B** and **D**). Tiron protected the virus for the first hour of contact, suggesting that superoxide generation is important. However, d-mannitol was minimally protective on copper but protected the virus for the duration of the test on brass. Increasing the concentration of d-mannitol did not prolong survival of infectivity on copper (not shown). This suggests that rapid inactivation of coronavirus on copper surfaces is primarily due to copper ion release and that the effect of reactive oxygen species is minimal. However, as the percentage of copper in the alloy decreased, ROS generation played a more significant role.

EDTA, BCS, d-mannitol, and Tiron did not significantly affect the virus on stainless steel control surfaces or in suspension (not shown).

**Inactivation of coronavirus on copper and copper alloy surfaces results in fragmentation of the viral genome, ensuring that inactivation is irreversible.**Coronavirus was exposed to metal surfaces and recovered, and the positive-stranded viral RNA genome was extracted and purified. A one-step reverse transcriptase real-time quantitative PCR (RTqPCR) was performed to detect a 139-bp region of ORF1 within nonstructural protein 4 (nsp4). Virus that had been exposed to copper and brass surfaces demonstrated reduced copy numbers of this fragment with increasing contact times

(Fig. 5A). Comparison of the entire viral genome by agarose gel electrophoresis confirmed that nonspecific fragmentation occurred on copper and brass, with fragments becoming smaller with increasing contact time (Fig. 5B).

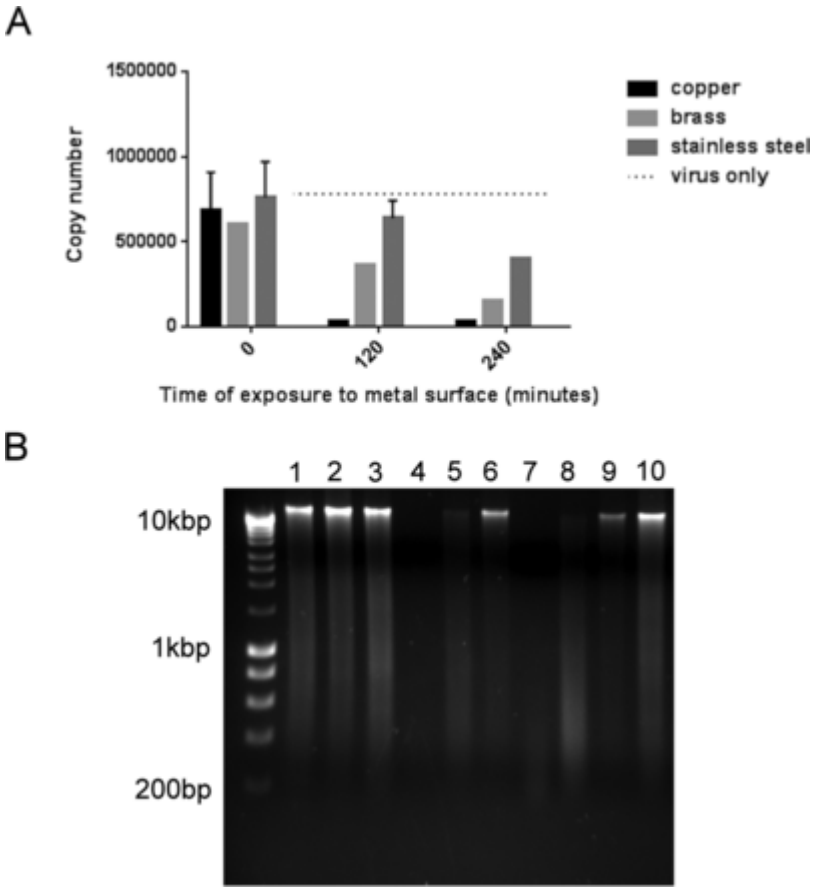


**FIG 5**

Destruction of human coronavirus viral genome on copper and copper alloy surfaces. (A) Analysis of a small fragment (136-bp region of the nsp4 gene) of the coronavirus genome revealed a reduction in copy number from virus exposed to copper and cartridge brass surfaces in reverse transcriptase real-time PCR. There was some reduction on stainless steel but none in viral suspension (lightest gray bars), suggesting that this was due to sample drying. (B) Analysis of the entire viral genome is represented in electrophoretic separation of viral RNA extracted from virus exposed to copper (lanes 1, 4, and 7), cartridge brass (lanes 2, 5, and 8), and stainless steel (lanes 3, 6, and 9) for 0 min (lanes 1 to 3), 120 min (lanes 4 to 6), and 240 min (lanes 7 to 9). The genomic RNA from virus exposed to copper and brass degraded with increased contact time. This did not occur on stainless steel; the genomic RNA remained as fragments too large to pass through the gel. However, the total amount of intact RNA was reduced at 4 h, possibly due to drying damage as seen in panel A. Lane 10 represents untreated virus, and the unmarked lane is a Bioline marker (Hyperladder I). The same procedure was used with mock-infected cells, revealing the same pattern of RNA breakdown following application to copper surfaces (not shown).

**Exposure to copper surfaces results in morphological changes to human coronavirus particles visible in transmission electron microscopy (TEM).**There was a significant difference in appearance between purified HuCoV-229E exposed to stainless steel and that exposed to copper surfaces (Fig. 6). On stainless steel, uniform virions were visible following a 10-min exposure (Fig. 6A), but on

copper, clumps of damaged virus particles (Fig. 6B) as well as a few intact particles could be seen. The extent of damage increased upon further exposure to copper (Fig. 6C).

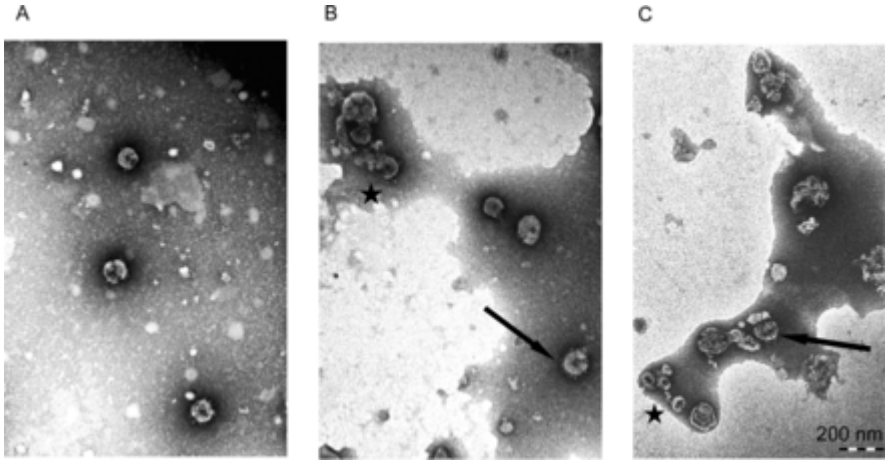


**FIG 6**

Exposure to copper surfaces results in morphological changes to human coronavirus. Purified HUCoV-229E was applied to metal surfaces and then removed, and a negatively stained preparation was observed using transmission electron microscopy. (A) Intact virions were visible following exposure to stainless steel for 10 min. (B) However, following exposure to copper for 10 min, many virus particles appeared to be disintegrating (indicated by a star), although some intact virions were still present (arrow). (C) After a 30-min exposure to copper, further damage had occurred and virions appeared shrunken (indicated by a star), with damage to surface spikes (arrow).

## DISCUSSION

A combination of genetic reassortment in viruses with segmented genomes and point mutations, particularly evident in viruses that cause disease in the respiratory tract such as influenza virus and coronaviruses, results in constantly changing antigenicity and host immune response evasion. This can also affect the attachment to the host cell receptor and the “host jump” from animals to human that can occur if the mutation results in an increased ability of the virus to bind to human cells. If this is accompanied by a decrease in binding to the original host, then human-to-human transmission can occur, presenting a substantial threat of rapid spread of a novel virus throughout the community (reviewed in reference 32).

Viruses causing respiratory infections are spread by droplets expelled by coughs and sneezes, which can also contaminate the environment 2 m and 6 m away, respectively (33), and a single droplet may easily contain an infectious dose (34). Enveloped respiratory viruses, although more susceptible to environmental stress than nonenveloped viruses, have been shown to persist on surfaces and contaminate more than 50% of surfaces in household and day care centers (35). Animal coronaviruses, including transmissible gastroenteritis virus (TGEV) and mouse hepatitis virus (MHV), have been shown to retain infectivity for long periods on hard surfaces (36) and for several hours on health care gowns, gloves, and masks (37), but human coronavirus 229E (HuCoV-229E) did not persist for above a few hours on surfaces (38). In contrast, we have observed that a relatively low titer of infectious human coronavirus 229E persisted on 5 surface materials, common to communal and domestic environments, for at least 5 days. Our virus preparation contained a high proportion of lung cell debris to mimic natural contamination in respiratory secretions, which may have protected the virus from desiccation, and a human lung cell line was used for the assay, which may have been more sensitive. The relatively low virus concentration used suggests that higher viral concentrations

which can occur in sputum may persist for longer periods. During coronavirus infection, the viral load is highest later in the infection and large numbers of infectious virus which may also contaminate the surrounding environment can be shed as symptoms subside over long periods (4). There is scant information on minimum infectious doses, but for many respiratory viruses, the minimum infectious dose is believed to be low, i.e., just a few virus particles. Coronavirus persistence on surfaces represents a considerable infection risk if contaminated surfaces are touched and infectious virus transferred to the mouth, nasal mucosa, or conjunctiva. Nicas and Best (39) observed that individuals in office environments touched their face an average of 15 times an hour, giving ample opportunities for infection spread. The use of antiviral surfaces in health care and community facilities could help to reduce infection spread in this way. HuCoV-229E was rapidly inactivated on copper surfaces, with the inactivation rate being roughly proportional to the percentage of copper in the alloy. Alloys containing >90% copper inactivated $10^3$ PFU coronavirus in <30 min, and a surface oxidation layer or increased copper ion release on C70600 increased efficacy, which has been observed for this alloy before (27). Brasses were more efficacious than copper nickels at a lower percentage of copper.

Previous studies by our laboratory have shown release of copper ionic species to be essential to the efficacy of copper surfaces in killing bacteria and inactivating norovirus (26). Using chelators, we have determined that Cu(I) and Cu(II) are also essential for inactivation of coronaviruses. On brass (70% copper), BCS, the chelator for Cu(I), was still protective at 2 h of contact, suggesting that inactivation may have been due to Cu(II) immediately and to Cu(I) in the long term. Copper ions have been shown to directly inhibit proteases by reacting with surface cysteine and to inflict damage to the viral genome in HIV and herpes simplex virus (40, 41).

The mechanism of bacterial death on copper surfaces is complex, involving not only direct action of copper ion on multiple targets but also the generation of destructive oxygen radicals, resulting in “metabolic suicide” (20). This was not observed for norovirus destruction on copper, presumably because of the lack of respiratory machinery (26). However, it appears that superoxide and hydroxyl radical generation may be important in the inactivation of coronaviruses on copper alloys but that inactivation on 100% copper surfaces is primarily due to the direct effect of copper ions. Following application of a wet droplet to a copper surface, the predominant ionic species to dissolute from the metal surface is Cu(II), but reduction to Cu(I) and the Fenton reaction with oxidative intermediates from cell debris, molecular oxygen, or viral envelope could produce the highly toxic hydroxyl radical. ROS are generated in the natural course of coronavirus infection (42) and contribute to pathogenesis and apoptosis. Fujimori et al. (43) observed inactivation of influenza A H1N1 pandemic 2009 strain by Cu(I) iodide nanoparticles which involved hydroxyl radicals and resulted in degradation of hemagglutinin and neuraminidase viral proteins. They surmised that, although there was no exogenous hydrogen peroxide to fuel the Fenton reaction (**equation 3**), Cu(I) reacted with molecular oxygen to generate superoxide (**equation 1**) and, subsequently, hydrogen peroxide (**equation 2**) (which could also produce hydroxyl radicals via the Haber Weiss reaction) as follows:

$$2Cu{+}{+}2O2(aq)\rightarrow 2Cu2{+}{+}2O2{-}2Cu{+}{+}2O2(aq)\rightarrow 2Cu2{+}{+}2O2{-}(1)2O2{-}{+}2H{+}\rightarrow H2O2+O22O2{-}{+}2H{+}\rightarrow H2O2+O2(2)Cu{+}{+}H2O2\rightarrow Cu2{+}{+}OH{-}{+}OH\cdot Cu{+}{+}H2O2\rightarrow Cu2{+}{+}OH{-}{+}OH\cdot(3)$$

In our results, the Cu(I) chelator BCS protected coronavirus on brass surfaces, suggesting that $Cu^+$ migrating from the metal is important in toxicity and supporting the Fenton reaction generation of hydroxyl radicals that was observed. Perhaps the reason brasses were more effective at inactivating coronavirus than copper nickels was the increased Cu(I) release and subsequent ROS generation rather than the zinc content, which had only mild antiviral activity. Presumably, as in bacteria, a multitarget attack on enveloped viruses by copper ions and ROS may result in

nonenzymatic peroxidation of the envelope (44) and damage to membrane proteins and the nucleoproteins.

We have observed previously (27) that exposure to copper surfaces resulted in significant morphological changes to nonenveloped norovirus, where possible disassociation of the capsid subunits exposed the viral genome to copper inactivation. In this study, we observed rapid damage, including clumping, breakage, membrane damage, and loss of surface spikes, to the coronavirus particles following exposure to copper, and some particles appeared smaller and seemed to have lost rigidity, folding up on themselves. These changes were not observed with virus recovered from stainless steel surfaces.

Analysis of coronavirus genomic RNA from viruses exposed to copper and copper alloys revealed a nonspecific fragmentation of the entire genome that can also be observed at the gene level by the reduction in copy number of a small fragment of nsp4 proteins, and the extent of damage increased with contact time. We have observed that the reduction in the capsid integrity of norovirus allows access of copper ions to the genome inactivating the virus. For coronavirus, the envelope and nucleoprotein are likewise compromised, and the process occurs more rapidly than with nonenveloped norovirus, which has a resistant capsid, to allow copper ion and/or ROS to destroy the genome. Interestingly, there was a 10-min delay in inactivation of simulated wet-droplet contamination which may reflect the time taken to breach the envelope and disrupt the nucleoprotein which allows access of copper ions to the coronavirus genome. Further studies may determine if the use of synergistic cleaning agents to weaken the envelope could reduce this delay. Sagripanti et al. (45) also reported increased sensitivity to solutions of copper ions of enveloped viruses compared to nonenveloped phages.

There are concerns about the pandemic potential of MERS, especially if the efficiency of interhuman transmission increases (46). The majority of cases have been in the Middle East, and concerns have been expressed because >2.5 million pilgrims attend the Hajj in Mecca, Saudi Arabia, aggregating from >180 countries. Analysis of data since June 2012 resulted in estimates that the risks of transmission are low (47, 48), but members of the Health Protection Agency (HPA) UK Novel Coronavirus Investigation team (49) have observed person-to-person transmission within a family cluster in the United Kingdom contracted from a family member who had visited Saudi Arabia. They also observed that the spectrum of symptoms of MERS, including mild and asymptomatic disease, is wider than initially realized and that spread of the virus may therefore already be greater than expected. MERS has so far killed 36 people and infected 186 patients in hospital-associated cases in South Korea associated with the first imported case arising from travel to the Middle East (10, 11). The current increase in the incidence of MERS has been described as a “subcritical epidemic,” but statistics have concentrated on severe cases only. It remains to be seen if the number of cases continues to escalate, and the evolution of SARS and MERS is a timely reminder of the constant threat of other coronaviruses making the jump from a large reservoir in wild and domestic animals to the human population. Several Hajj pilgrims returning to Austria had contracted serious respiratory disease caused by influenza A and B virus and not MERS (50), emphasizing that there are multiple risks of contacting infectious diseases in any highly populated areas.

The results from this study have shown that a relatively low concentration of enveloped respiratory viruses may retain infectivity on common hard surfaces for longer than previously thought and may present a real risk of infection to anyone who contacts a contaminated surface. However, human coronavirus 229E, an important pathogenic virus but also a surrogate for MERS coronavirus, which is structurally very similar, was rapidly inactivated on copper alloys. Inactivation results from a combination of direct copper ion attack and reactive oxygen species generation. The latter is

particularly important as the copper content decreases, ensuring that rapid inactivation still occurs in alloys with lower percentages of copper. Therefore, incorporation of copper alloys in communal areas could help to reduce infection spread from touching surfaces contaminated with coronaviruses. This is especially important in infectious disease where the infectious dose is low, surface contamination is high, and effective therapies are limited. The mechanism of action of copper is complex and may be enhanced by radical formation but is ultimately nonspecific, ensuring continuous kill and inactivation of a wide range of pathogenic microorganisms with completely different morphologies. Concerns about the biocide resistance, possible concomitant drug resistance, and horizontal gene transfer that have been observed with other biocides (**51**) can be allayed because of the destruction of viral nucleic acid observed following exposure to copper surfaces. It is not feasible to cover every surface in copper, and many materials in the built environment, including stainless steel, will continue to be used because of resilience, anticorrosion, and other beneficial attributes. Incorporation of even a few copper surfaces may have an impact in effectively reducing transmission of infectious material from a surface to an individual, provided that stringent, regular, and effective cleaning regimens are employed for all surfaces. The use of copper does not serve as an excuse to relax cleaning regimens. However, the choice of cleaning reagents is critical for copper alloys because it is essential to maintain copper ion release for efficacy, so avoidance of chelators is necessary.

There is now a large body of evidence from laboratory studies and small clinical trials to suggest that incorporation of copper surfaces could play a significant role in reducing infection transmission from contaminated surfaces. The time is nigh to investigate this further on a larger scale, but fears of the installation costs appear to be hampering the progress. Given the huge costs, human and monetary, associated with the treatment and care of patients with hospital-acquired infections, preliminary studies have suggested that the initial costs could be recouped within a few months (**52**). New technologies in copper coatings are being developed which may allow large-scale community areas, such as transport facilities, to be rendered antimicrobial at reduced costs. A note of caution: for these to be effective, there must be actual contact between copper and the contaminating pathogenic microorganisms, because any interference from matrix components could result in false economy.

## MATERIALS AND METHODS

**Viral strains and cell lines.**Human coronavirus 229E (HuCoV-229E) and a fetal fibroblast cell line, MRC-5, were supplied by Public Health England (PHE), United Kingdom. Cells were maintained in minimal essential medium (MEM) supplemented with GlutaMax-1, nonessential amino acids, and 5% fetal calf serum and incubated at 37°C and 5% $CO_2$. Cells were passaged twice a week using trypsin (0.25%)-EDTA and were not used beyond passage 30 (P30) (which occurred before the onset of senescence, but susceptibility to infection diminished greatly from P30). Viral stocks were prepared by infecting cells at multiplicity of infection of 0.01 for 4 to 7 days until a significant cytopathic effect (CPE) was observed. Infected cells were subjected to 3 freeze/thaw cycles, and infected-cell lysate was stored at −80°C.

**Preparation of sample surfaces.**Metal coupons (10 by 10 by 0.5 mm) were degreased in acetone, stored in absolute ethanol, and flamed prior to use as described previously (**19**). Metal samples were supplied by the Copper Development Association and are described in **Table 1**. Coupons of nonmetal surfaces (PTFE, polyvinyl chloride [PVC], ceramic tiles, glass, and silicone rubber) of the same size were sterilized by autoclaving at 121°C and $1.06 \times 10^5$ pascals (1.06 bar) for 15 min. Stainless steel controls for comparison were also autoclaved for method consistency for these experiments.

**Infectivity assay for HuCoV-229E exposed to surfaces.**Infected cell lysate preparations of HuCoV-229E were spread over coupons of the test surface and incubated at room temperature. The virus was removed from the coupons at various times and assayed for infectious virus by a plaque assay which was a modification of the murine norovirus 1 (MNV-1) assay described previously (**26**). Briefly, coupons inoculated with virus and incubated for various times at room temperature were added to a tube containing 5 ml growth medium and 2-mm-diameter glass beads and subjected to vortex mixing for 15 s. Dilutions were prepared in growth medium, and 1-ml aliquots were plated onto confluent monolayers of MRC-5 cells that had been prepared 24 h earlier in 6-well trays. The inoculum was removed after 90 min and replaced with agarose overlays, and plates were incubated at 37°C and 5% $CO_2$ for 4 to 7 days until CPE was evident. The monolayers were stained with vital stain and neutral red, and plaques in the monolayer were enumerated. Triplicate samples were processed for each time point.

**The effect of copper chelators and reactive oxygen species quenchers on infectivity of human coronavirus exposed to copper and copper alloy surfaces.**Incorporation of chelators ethylenediaminetetraacetic acid (EDTA) (20 mM) and bathocuproine disulfonic acid (BCS) (20 mM) to chelate Cu(II) and Cu(I), respectively, at the time of inoculation of virus onto the metal surfaces was investigated using a plaque assay. In addition, 20 mM d-mannitol and 20 mM Tiron (4,5-dihydroxy-1,3-benzene disulfonic acid) were used to quench hydroxyl radicals and superoxide, respectively. Stainless steel was used as a control surface and to determine if quenchers and chelators affect viral replication.

**Purification of viral RNA and analysis of integrity by agarose gel electrophoresis.**The total RNA of untreated virus or virus exposed to metal surfaces (5 coupons per test, with virus removed from coupons by pipetting up and down in a small volume [100 µl]) was extracted using a Qiagen QIAamp viral RNA minikit according to the manufacturer's instructions and the carrier RNA provided to prevent degradation.

Purified RNA fragments were separated on a nondenaturing 1% agarose gel using a GelRed nucleic acid prestaining kit (Biotium, United Kingdom) according to the manufacturer's instructions. The staining intensity is reduced because GelRed binds to single-stranded RNA (ssRNA) approximately half as much as to double-stranded nucleic acid. DNA ladders were supplied by Bioline. Gels were observed and photographed using GeneSnap software and a Syngene UV light box.

**Detection and quantification of a 139-bp region of the coronavirus nonstructural gene encoding nsp4 in virus exposed to copper and brass surfaces.**To determine if exposure to copper affected the viral genome at the gene level, a 139-bp region of the gene encoding nsp4 (within polyprotein 1ab replicase) was investigated using a One-Step real-time quantitative PCR (RTqPCR) diagnostic kit (supplied by PrimerDesign, United Kingdom). The kit is based on sequences from HuCoV-229E (GenBank accession number NC_002645; anchor nucleotide position 8205). Amplification was performed on a BioRad iQ5 cycler, and standard curves were prepared from known copy number standards to determine copy numbers in test samples. PCR products were analyzed by gel electrophoresis as described above.

**Detection of morphological changes to HuCoV-229E using transmission electron microscopy (TEM).**HuCoV-229E was purified from crude infected-cell lysate. Polyethylene glycol (PEG) precipitation (BioVision PEG virus precipitation kit) was followed by sucrose density (25% to 55%) centrifugation at 96,000 × *g* for 16 h at 4°C. The virus band was resuspended in water and the virus pelleted at 77,000 × *g* for 1 h at 4°C. The supernatant was discarded, the tubes were allowed to drain, and the final pellet was resuspended in ice-cold nuclease-free deionized distilled water after

incubation on ice for 30 min. The preparation was applied to copper and stainless steel as described in the **Figure 6** legend and was removed by gentle pipetting. Samples were fixed, applied to TEM grids, washed with water, and stained with 5% ammonium molybdate for 10 s.

**Statistical analysis.**Data are expressed as means ± standard errors of the mean (SEM) and are from the results of multiple independent experiments. Statistical analyses and representational graphic depictions were performed using GraphPad Prism 6.

**ACKNOWLEDGMENTS**

This research was supported by the Copper Development Association, New York, and the International Copper Association, New York.

We thank Anton Page, Patricia Goggin, Lizzie Angus, and everyone at the Biomedical Imaging Unit, University of Southampton, Southampton, United Kingdom, for their help with the use of the transmission electron microscope.

**FOOTNOTES**

- Received 1 October 2015
- Accepted 13 October 2015
- Published 10 November 2015



**REFERENCES**

1. 1.↲

    1. Zambon M

. 2014. Influenza and other emerging respiratory viruses. Medicine **42**:45–51 doi:10.1016/j.mpmed.2013.10.017.

**CrossRefGoogle Scholar**

2. 2.↲

    1. Ruuskanen O,
    2. Lahti E,
    3. Jennings LC,
    4. Murdoch DR

. 2011. Viral pneumonia. Lancet **377**:1264–1275. doi:10.1016/S0140-6736(10)61459-6.

**CrossRefPubMedWeb of ScienceGoogle Scholar**

3. 3.↲

1. Van den Brand JM,
2. Smits SL,
3. Haagmans BL

. 2015. Pathogenesis of Middle East respiratory syndrome coronavirus. J Pathol **235**:175–184. doi:10.1002/path.4458.

**CrossRefPubMedGoogle Scholar**

4. 4.↲

1. Gralinski LE,
2. Baric RS

. 2015. Molecular pathology of emerging coronavirus infections. J Pathol **235**:185–195. doi:10.1002/path.4454.

**CrossRefPubMedGoogle Scholar**

5. 5.↲

1. Coleman CM,
2. Frieman MB

. 2014. Coronaviruses: important emerging human pathogens. J Virol **88**:5209–5212. doi:10.1128/JVI.03488-13.

**Abstract/FREE Full TextGoogle Scholar**

6. 6.↲

1. Chan JFW,
2. Lau SKP,
3. To KKW,
4. Cheng VCC,
5. Woo PCY,
6. Yuen K

. 2015. Middle East respiratory syndrome coronavirus: another zoonotic betacoronavirus causing SARS-like disease. Clin Microbiol Rev **28**:465–522. doi:10.1128/CMR.00102-14.

**Abstract/FREE Full TextGoogle Scholar**

7. 7.↲

1. Cong Y,
2. Ren X

. 2014. Coronavirus entry and release in polarized epithelial cells: a review. Rev Med Virol **24**:308–315. doi:10.1002/rmv.1792.

CrossRefPubMedGoogle Scholar

8. 8.↲

    1. Hemida MG,
    2. Al-Naeem A,
    3. Perera RAPM,
    4. Chin AWH,
    5. Poon LLM,
    6. Peiris M

. 2015. Lack of Middle East respiratory syndrome coronavirus transmission from infected camels. Emerg Infect Dis **21**:699–701. doi:10.3201/eid2104.141949.

CrossRefGoogle Scholar

9. 9.↲

    1. Oboho IK,
    2. Tomczyk SM,
    3. Al-Asmari AM,
    4. Banjar AA,
    5. Al-Mugti H,
    6. Aloraini MS,
    7. Alkhaldi KZ,
    8. Almohammadi EL,
    9. Alraddadi BM,
    10. Gerber SI,
    11. Swerdlow DL,
    12. Watson JT,
    13. Madani TA

. 2015. 2014 MERS-CoV outbreak in Jeddah—a link to health care facilities. N Engl J Med **372**:846–854. doi:10.1056/NEJMoa1408636.

CrossRefPubMedGoogle Scholar

10. 10.↲

    1. Butler D.

2015. South Korean MERS outbreak spotlights lack of research. Nature **522**:139–140. doi:10.1038/522139a.

CrossRefPubMedGoogle Scholar

11. 11.↲

    1. Ki M

. 2015. 2015 MERS outbreak in Korea: hospital-to-hospital transmission. Epidemiol Health **37**:e2015033. doi:10.4178/epih/e2015033.

CrossRefPubMedGoogle Scholar

12. 12.↲

    1. Otter JA,
    2. Yezli S,
    3. Salkeld JAG,
    4. French GL

. 2013. Evidence that contaminated surfaces contribute to the transmission of hospital pathogens and an overview of strategies to address contaminated surfaces in hospital settings. Am J Infect Control **41**:S6–S11. doi:10.1016/j.ajic.2012.12.004.

CrossRefPubMedGoogle Scholar

13. 13.↲

    1. Bean B,
    2. Moore BM,
    3. Sterner B,
    4. Peterson LR,
    5. Gerding DN,
    6. Balfour HH, Jr..

1982. Survival of influenza viruses on environmental surfaces. J Infect Dis **146**:47–51. doi:10.1093/infdis/146.1.47.

CrossRefPubMedWeb of ScienceGoogle Scholar

14. 14.↲

    1. Wilks SA,
    2. Michels H,
    3. Keevil CW

. 2005. The survival of *Escherichia coli* O157 on a range of metal surfaces. Int J Food Microbiol **105**:445–454. doi:10.1016/j.ijfoodmicro.2005.04.021.

CrossRefPubMedWeb of ScienceGoogle Scholar

15. 15.↲

1. Noyce JO,
2. Michels H,
3. Keevil CW

. 2006. Potential use of copper surfaces to reduce survival of epidemic meticillin-resistant *Staphylococcus aureus* in the healthcare environment. J Hosp Infect **63**:289–297. doi:10.1016/j.jhin.2005.12.008.

**CrossRefPubMedWeb of ScienceGoogle Scholar**

16. 16.↲

1. Noyce JO,
2. Michels H,
3. Keevil CW

. 2006. Use of copper cast alloys to control *Escherichia coli* O157 cross-contamination during food processing. Appl Environ Microbiol **72**:4239–4244. doi:10.1128/AEM.02532-05.

**Abstract/FREE Full TextGoogle Scholar**

17. 17.↲

1. Weaver L,
2. Michels HT,
3. Keevil CW

. 2008. Survival of *Clostridium difficile* on copper and steel: futuristic options for hospital hygiene. J Hosp Infect **68**:145–151. doi:10.1016/j.jhin.2007.11.011.

**CrossRefPubMedWeb of ScienceGoogle Scholar**

18. 18.↲

1. Weaver L,
2. Michels HT,
3. Keevil CW

. 2010. Potential for preventing spread of fungi in air-conditioning systems constructed using copper instead of aluminium. Lett Appl Microbiol **50**:18–23. doi:10.1111/j.1472-765X.2009.02753.x.

**CrossRefPubMedGoogle Scholar**

19. 19.↲

1. Warnes SL,
2. Green SM,
3. Michels HT,
4. Keevil CW

. 2010. Biocidal efficacy of copper alloys against pathogenic enterococci involves degradation of genomic and plasmid DNAs. Appl Environ Microbiol **76**:5390–5401. doi:10.1128/AEM.03050-09.

**Abstract/FREE Full TextGoogle Scholar**

20. 20.↲

    1. Warnes SL,
    2. Keevil CW

. 2011. Mechanism of copper surface toxicity in vancomycin-resistant enterococci following wet or dry surface contact. Appl Environ Microbiol **77**:6049–6059. doi:10.1128/AEM.00597-11.

**Abstract/FREE Full TextGoogle Scholar**

21. 21.↲

    1. Warnes SL,
    2. Caves V,
    3. Keevil CW

. 2012. Mechanism of copper surface toxicity in *Escherichia coli* O157:H7 and *Salmonella* involves immediate membrane depolarization followed by slower rate of DNA destruction which differs from that observed for Gram-positive bacteria. Environ Microbiol **14**:1730–1743. doi:10.1111/j.1462-2920.2011.02677.x.

**CrossRefPubMedGoogle Scholar**

22. 22.↲

    1. Casey AL,
    2. Adams D,
    3. Karpanen TJ,
    4. Lambert PA,
    5. Cookson BD,
    6. Nightingale P,
    7. Miruszenko L,
    8. Shillam R,
    9. Christian P,
    10. Elliott TSJ

. 2010. Role of copper in reducing hospital environment contamination. J Hosp Infect **74**:72–77. doi:10.1016/j.jhin.2009.08.018.

**CrossRefPubMedGoogle Scholar**

23. 23.↲

1. Karpanen TJ,
2. Casey AL,
3. Lambert PA,
4. Cookson BD,
5. Nightingale P,
6. Miruszenko L,
7. Elliott TSJ

. 2012. The antimicrobial efficacy of copper alloy furnishing in the clinical environment: a crossover study. Infect Control Hosp Epidemiol **33**:3–9. doi:10.1086/663644.

CrossRefPubMedGoogle Scholar

24. 24.↲

1. Schmidt MG,
2. Attaway HH,
3. Sharpe PA,
4. John J, Jr.,
5. Sepkowitz KA,
6. Morgan A,
7. Fairey SE,
8. Singh S,
9. Steed LL,
10. Cantey JR,
11. Freeman KD,
12. Michels HT,
13. Salgado CD

. 2012. Sustained reduction of microbial burden on common hospital surfaces through introduction of copper. J Clin Microbiol **50**:2217–2223. doi:10.1128/JCM.01032-12.

Abstract/FREE Full TextGoogle Scholar

25. 25.↲

1. Salgado CD,
2. Sepkowitz KA,
3. John JF,
4. Cantey JR,

5. Attaway HH,
6. Freeman KD,
7. Sharpe PA,
8. Michels HT,
9. Schmidt MG

. 2013. Copper surfaces reduce the rate of healthcare-acquired infections in the intensive care unit. Infect Control Hosp Epidemiol **34**:479–486. doi:10.1086/670207.

CrossRefPubMedGoogle Scholar

26. 26.↲

1. Warnes SL,
2. Keevil CW

. 2013. Inactivation of norovirus on dry copper alloy surfaces. PLoS One **8**:e75017. doi:10.1371/journal.pone.0075017.

CrossRefPubMedGoogle Scholar

27. 27.↲

1. Warnes SL,
2. Summersgill EN,
3. Keevil CW

. 2015. Inactivation of murine norovirus on a range of copper alloy surfaces is accompanied by loss of capsid integrity. Appl Environ Microbiol **81**:1085–1091. doi:10.1128/AEM.03280-14.

Abstract/FREE Full TextGoogle Scholar

28. 28.↲

1. Manuel CS,
2. Moore MD,
3. Jaykus LA

. 2015. Destruction of the capsid and genome of GII.4 human norovirus occurs during exposure to metal alloys containing copper. Appl Environ Microbiol **81**:4940–4946. doi:10.1128/AEM.00388-15.

Abstract/FREE Full TextGoogle Scholar

29. 29.↲

1. Pene F,
2. Merlat A,
3. Vabret A,

4. Rozenberg F,
5. Buzyn A,
6. Dreyfus F,
7. Cariou A,
8. Freymuth F,
9. Lebon P

. 2003. Coronavirus 229E-related pneumonia in immunocompromised patients. Clin Infect Dis **37**:929–932. doi:10.1086/377612.

CrossRefPubMedWeb of ScienceGoogle Scholar

30. 30.↲
    1. Boucher A,
    2. Desforges M,
    3. Duquette P,
    4. Talbot PJ

. 2007. Long-term human coronavirus-myelin cross-reactive T-cell clones derived from multiple sclerosis patients. Clin Immunol **123**:258–267. doi:10.1016/j.clim.2007.02.002.

CrossRefPubMedWeb of ScienceGoogle Scholar

31. 31.↲
    1. Corman VM,
    2. Baldwin HJ,
    3. Fumie TA,
    4. Melim ZR,
    5. Annan A,
    6. Owusu M,
    7. Nkrumah EE,
    8. Maganga GD,
    9. Oppong S,
    10. Adu-Sarkodie Y,
    11. Vallo P,
    12. da Silva Filho LV,
    13. Leroy EM,
    14. Thiel V,

15. van der Hoek L,
16. Poon LL,
17. Tschapka M,
18. Drosten C,
19. Drexler JF

. 16 September 2015. Evidence for an ancestral association of human coronavirus 229E with bats. J Virol doi:10.1128/JVI.01755-15.

**Abstract/FREE Full TextGoogle Scholar**

32. 32.↲

1. Shi Y,
2. Wu Y,
3. Zhang W,
4. Qi J,
5. Gao GF

. 2014. Enabling the “host jump”: structural determinants of receptor-binding specificity in influenza A viruses. Nat Rev Microbiol **12**:822–831. doi:10.1038/nrmicro3362.

**CrossRefPubMedGoogle Scholar**

33. 33.↲

1. Xie X,
2. Li Y,
3. Chwang ATY,
4. Ho PL,
5. Seto WH

. 2007. How far droplets can move in indoor environments—revisiting the wells evaporation-falling curve. Indoor Air **17**:211–225. doi:10.1111/j.1600-0668.2007.00469.x.

**CrossRefPubMedWeb of ScienceGoogle Scholar**

34. 34.↲

1. Yezli S,
2. Otter JA

. 2011. Minimum infective dose of the major respiratory and enteric viruses transmitted through food and the environment. Food Environ Virol **3**:1–30. doi:10.1007/s12560-011-9056-7.

**CrossRefGoogle Scholar**

35. 35.↲

1. Boone S,
2. Gerba C

. 2005. The occurrence of influenza A virus on household and day care center fomites. J Infect **51**:103–109. doi:10.1016/j.jinf.2004.09.011.

CrossRefPubMedWeb of ScienceGoogle Scholar

36. 36.↲

1. Casanova LM,
2. Jeon S,
3. Rutala WA,
4. Weber DJ,
5. Sobsey MD

. 2010. Effects of air temperature and relative humidity on coronavirus survival on surfaces. Appl Environ Microbiol **76**:2712–2717. doi:10.1128/AEM.02291-09.

Abstract/FREE Full TextGoogle Scholar

37. 37.↲

1. Casanova L,
2. Rutala W,
3. Weber D,
4. Sobsey M

. 2010. Coronavirus survival on healthcare personal protective equipment. Infect Control Hosp Epidemiol **31**:560–561. doi:10.1086/652452.

CrossRefPubMedGoogle Scholar

38. 38.↲

1. Sizun J,
2. Yu MWN,
3. Talbot PJ

. 2000. Survival of human coronaviruses 229E and OC43 in suspension and after drying on surfaces: a possible source of hospital-acquired infections. J Hosp Infect **46**:55–60. doi:10.1053/jhin.2000.0795.

CrossRefPubMedWeb of ScienceGoogle Scholar

39. 39.↲

1. Nicas M,

2. Best D

. 2008. A study quantifying the hand-to-face contact rate and its potential application to predicting respiratory tract infection. J Occup Environ Hyg **5**:347–352. doi:10.1080/15459620802003896.

CrossRefPubMedWeb of ScienceGoogle Scholar

40. 40.↲

1. Karlstrom AR,
2. Levine RL

. 1991. Copper inhibits the protease from human immunodeficiency virus 1 by both cysteine-dependent and cysteine-independent mechanisms. Proc Natl Acad Sci U S A **88**:5552–5556. doi:10.1073/pnas.88.13.5552.

Abstract/FREE Full TextGoogle Scholar

41. 41.↲

1. Sagripanti JL,
2. Routson LB,
3. Bonifacino AC,
4. Lytle CD

. 1997. Mechanism of copper-mediated inactivation of herpes simplex virus. Antimicrob Agents Chemother **41**:812–817.

Abstract/FREE Full TextGoogle Scholar

42. 42.↲

1. Ding L,
2. Zhao X,
3. Huang Y,
4. Du Q,
5. Dong F,
6. Zhang H,
7. Song X,
8. Zhang W,
9. Tong D

. 2013. Regulation of ROS in transmissible gastroenteritis virus-activated apoptotic signaling. Biochem Biophys Res Commun **442**:33–37. doi:10.1016/j.bbrc.2013.10.164.

CrossRefPubMedGoogle Scholar

43. 43.↲

1. Fujimori Y,
2. Sato T,
3. Hayata T,
4. Nagao T,
5. Nakayama M,
6. Nakayama T,
7. Sugamata R,
8. Suzuki K

. 2012. Novel antiviral characteristics of nanosized copper(I) iodide particles showing inactivation activity against 2009 pandemic H1N1 influenza virus. Appl Environ Microbiol **78**:951–955. doi:10.1128/AEM.06284-11.

**Abstract/FREE Full TextGoogle Scholar**

44. 44.↲

1. Hong R,
2. Kang TY,
3. Michels CA,
4. Gadura N

. 2012. Membrane lipid peroxidation in copper alloy-mediated contact killing of *Escherichia coli*. Appl Environ Microbiol **78**:1776–1784. doi:10.1128/AEM.07068-11.

**Abstract/FREE Full TextGoogle Scholar**

45. 45.↲

1. Sagripanti JL,
2. Routson LB,
3. Lytle CD

. 1993. Virus inactivation by copper or iron ions alone and in the presence of peroxide. Appl Environ Microbiol **59**:4374–4376.

**Abstract/FREE Full TextGoogle Scholar**

46. 46.↲

1. Booth T,
2. Kournikakis B,
3. Bastien N,
4. Ho J,

5. Kobasa D,
6. Stadnyk L,
7. Li Y,
8. Spence M,
9. Paton S,
10. Henry B,
11. Mederski B,
12. White D,
13. Low D,
14. McGeer A,
15. Simor A,
16. Vearncombe M,
17. Downey J,
18. Jamieson F,
19. Tang P,
20. Plummer F

. 2005. Detection of airborne severe acute respiratory syndrome (SARS) coronavirus and environmental contamination in SARS outbreak units. J Infect Dis **191**:1472–1477. doi:10.1086/429634.

**CrossRefPubMedWeb of ScienceGoogle Scholar**

47. 47.↲

1. Breban R,
2. Riou J,
3. Fontanet A

. 2013. Interhuman transmissibility of Middle East respiratory syndrome coronavirus: estimation of pandemic risk. Lancet **382**:694–699. doi:10.1016/S0140-6736(13)61492-0.

**CrossRefGoogle Scholar**

48. 48.↲

1. Soliman T,
2. Cook AR,
3. Coker RJ

. 2015. Pilgims and MERS-CoV: what's the risk? Emerg Themes Epidemiol **12**:3. doi:10.1186/s12982-015-0025-8.

CrossRefPubMedGoogle Scholar

49. 49.↲

    1. Health Protection Agency (HPA) UK Novel Coronavirus Investigation team

. 2013. Evidence of person-to-person transmission within a family cluster of novel coronavirus infections, United Kingdom, February 2013. Euro Surveill **18**:20427.

PubMedGoogle Scholar

50. 50.↲

    1. Aberle JH,
    2. Popow-Kraupp T,
    3. Kreidl P,
    4. Laferl H,
    5. Heinz FX,
    6. Aberle SW

. 2015. Influenza A and B viruses but not MERS-CoV in Hajj pilgrims, Austria, 2014. Emerg Infect Dis **21**:726–727. doi:10.3201/eid2104.141745.

CrossRefPubMedGoogle Scholar

51. 51.↲

    1. Webber MA,
    2. Whitehead RN,
    3. Mount M,
    4. Loman NJ,
    5. Pallen MJ,
    6. Piddock LJV

. 2015. Parallel evolutionary pathways to antibiotic resistance selected by biocide exposure. J Antimicrob Chemother **70**:2241–2248. doi:10.1093/jac/dkv109.

CrossRefPubMedGoogle Scholar

52. 52.↲

    1. Michels HT,
    2. Keevil CW,
    3. Salgado CD,

4. Schmidt MG

. 2015. From laboratory research to a clinical trial: copper alloy surfaces kill bacteria and reduce hospital-acquired infections. HERD **9**:64–79. doi:10.1177/1937586715592650.

**CrossRefPubMedGoogle Scholar**